energies

MDPI

Article

Field Test of Superheater Pipes Vibration Caused by Sound Energy in the 235 MW_e Circulating Fluidized Bed Boiler

Paweł Mirek

Department of Advanced Energy Technologies, Faculty of Infrastructure and Environment, Czestochowa University of Technology, 42-201 Czestochowa, Poland; pawel.mirek@pcz.pl; Tel.: +48-343-250-933

Abstract: This paper presents the results of measurements of vibrations of the pipes of the steam superheater installed in the convection pass of the 235 MW_e Circulating Fluidized Bed boiler (CFB) induced using sonic soot blowers of the Nirafon NI-100 type. The measurements were made using two ICP Triaxial 356A16 accelerometers allowing the analysis of accelerations in the maximum range of ± 490 m/s^2. Simultaneously with vibration measurements, the sound pressure level was recorded using the G.R.A.S. 40BH high-pressure microphone. The measurements and spectral analysis of the recorded signals showed that the acoustic wave of 148 dB is safe for the steam superheater pipes causing vibrations of maximum amplitude not exceeding 1 mm. The field tests confirmed the supposition that the dominant mechanism for cleaning the surfaces of the superheater's heating pipes are not pipe vibrations, but the breakage of cohesion forces between dust particles.

Keywords: sonic soot blowers; ash deposits; superheaters; circulating fluidized bed; vibration

Citation: Mirek, P. Field Test of Superheater Pipes Vibration Caused by Sound Energy in the 235 MW_e Circulating Fluidized Bed Boiler. *Energies* **2021**, *14*, 7678. https://doi.org/10.3390/en14227678

Academic Editor: Jose A. Almendros-Ibanez

Received: 13 October 2021
Accepted: 15 November 2021
Published: 16 November 2021

1. Introduction

One of the basic operational problems of Circulating Fluidized Bed (CFB) boilers fired with solid fuels is the formation of troublesome ash deposits. Their chemical composition and quantity result directly from the type of fuel and particularly the ash content [1]. Ash, which is an inherent product of thermal fuel conversion and is deposited on the boiler's heating surfaces, acts as insulation in the heat exchange process, inhibiting the flow of heat from the flue gas to the circulating medium in the water and steam system. As a result, the thermal efficiency of the boiler and its availability decreases, which in extreme cases may even lead to a complete blockage of the flue gas ducts, making it necessary to temporarily shut down the unit. Estimated annual costs caused by ash sludge in the United States of America amount to $1.2 billion [2,3].

Ash deposits in boilers are usually classified into two categories: slagging, occurring when radiation is the dominant heat exchange mechanism [4], and fouling, when convection is the dominant heat exchange mechanism [5]. For this reason, the combustion chamber is a typical location for fused deposits, while convective passes are typical areas for sintered deposits. The effectiveness of the removal of ash deposits occurring in the convective pass depends on many factors resulting from: the construction of the soot blower (e.g., nozzle design, operating pressure, steam flow rate) and deposit characteristics (e.g., thickness, intergranular bond strength) [1]. Ensuring the maximum thermal efficiency of the boiler requires the effective removal of ash deposits. Both natural and artificial ash removal mechanisms play an active role in this process (Figure 1). In boilers burning solid fuels, natural mechanisms include gravity shedding, erosion, and thermal shock play a crucial role [6].

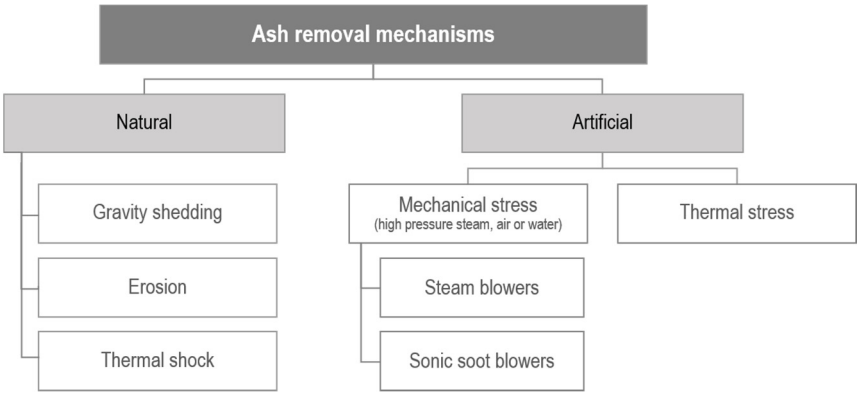

Figure 1. Ash removal mechanisms in CFB boilers.

The chemical composition of the ash will be the main factor determining which of the mechanisms will play a key role in the deposit disposal process. In most cases, ash deposits must be removed artificially by mechanical or thermal stress. This is done with the use of a stream of steam, air, or water under high pressure with a simultaneous change of thermal load [6]. In CFB boilers fired with hard coal and lignite, the heating surfaces placed in the convection pass are usually cleaned mechanically using steam blowers. The popularity of these devices is mainly due to their high efficiency and the parameters of the working medium (1.5–4.0 MPa; 673–773 K). However, according to the operating experience, these devices, apart from high operating costs [7–10], are also the source of many problems. The most serious is the erosive impact of ash entrained with the steam stream (Figure 2) [11]. Another problem is insufficient surface cleaning in places inaccessible to steam, shown in Figure 2 [12].

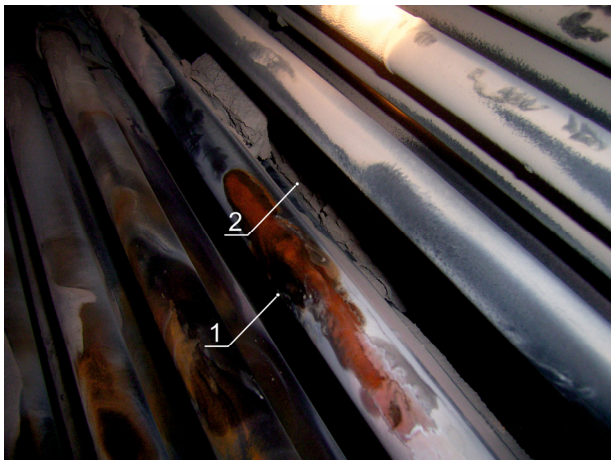

Figure 2. Superheater pipes in the 235 MW_e CFB boiler operating in the PGE GiEK S.A. Turów Power Plant, Poland. (1) Failure caused by the erosive impact of ash entrained with the steam jet of a soot blower; (2) ash deposit in an inaccessible place to the deposit-removing medium.

Therefore, in recent years there has been an increased interest in the use of non-invasive effective deposit-removal systems, based on high sound intensity (140–170 dB) and low frequency (60–150 Hz). The source of such a wave is the sonic soot blower supplied by compressed air or liquid gas. The operation of these devices consists in the short-term (1–10 s) emission of an acoustic wave of high sound pressure level and low frequency. The energy of this wave on the one hand causes the vibrating movement of dust particles carried in the flue gas stream, preventing their agglomeration, and on the other hand, prevents the formation of high-temperature deposits. Optimal cleaning effects depend mainly on: dust properties, dust distribution in the convection pass, sound

pressure level, supply air pressure, and the operating characteristics of the sonic soot blower. In practice, the efficiency of the acoustic blowers is assessed by measuring the temperature of the flue gas or the medium flowing through the heat transfer system, or by visual observations of the heated surfaces during operation or when the boiler is at shut-down. As the operating efficiency of the acoustic cleaners increases at low frequencies, the exposure of freely suspended pipes of superheaters placed in the convection pass to high energy waves carries a high risk of mechanical damage. Estimation of such risk is possible only based on measurements of heat transfer surface vibrations made on the object during the boiler shutdown.

Considering the growing interest in the use of non-invasive methods of removing ash deposits from the heat transfer surfaces in CFB boilers in recent years, two objectives of this work were formulated. From an operational point of view, the aim is to determine the magnitude of the vibration induced by the acoustic wave, which is very significant in the safe and unproblematic operation of the boiler. On the other hand, from a scientific point of view, the goal is to determine the particle removal mechanism accompanying the generation of high energy sound waves. The paper presents the results of measurements of vibrations of the pipes of the convection steam superheater located in the convection pass of the 235 MW_e CFB boiler induced using sound energy generated by sonic soot blowers of the Nirafon NI-100 type. The measurements have been made using two piezoelectric accelerometers and a special microphone with an extended measuring range up to 194 dB. The novelty of the conducted research consists in a comprehensive approach to the assessment of the impact of acoustic waves of high energy on the heated surfaces located in the second pass of the CFB boiler by simultaneously measuring the intensity of the acoustic wave, its frequency spectrum, and vibrations of steam superheater pipes. The lack of previous literature reports in this regard is justified by the very high risk of health loss during measurements resulting from the high energy of the acoustic wave. Therefore, the presented results are unique and represent the first attempt to assess the impact of acoustic waves on the heating surfaces of the CFB boiler.

2. Experimental Tests

Experimental tests have been carried out during the shutdown of the 235 MW_e CFB boiler operating in PGE GiEK S.A. Turów Power Plant, Poland. The boiler combustion chamber at the fluidizing grid level is 21.2 m long and 5.2 m wide, with the width growing with increasing distance from the grid. At the height of 6.7 m, the combustion chamber width is 9.9 m and does not change with a further increase of the distance from the grid. The total height of the combustion chamber is equal to 44.8 m. The boiler is fired with brown coal. Figure 3 shows the particle size distribution of a fly ash flowing through the convection pass of the boiler.

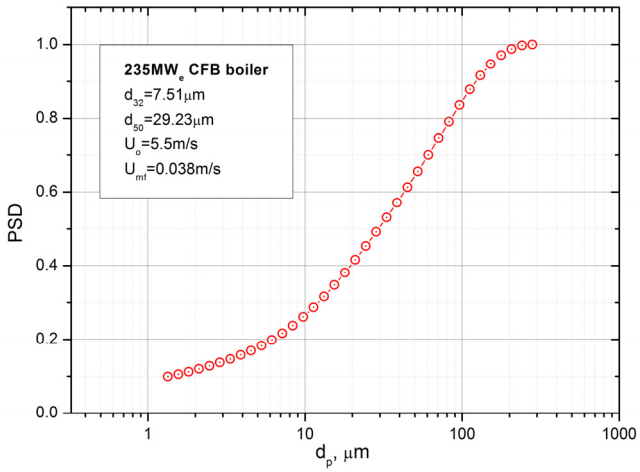

Figure 3. Particle size distribution of a fly ash flowing through the convection pass of the boiler.

Before the tests, the boiler was running under operating conditions, parameters of which are presented in Table 1. Table 2 presents the characteristics of a fuel and a sorbent.

Table 1. Operational parameters of the 235 MW_e CFB boiler.

General	Unit	Value
Electric power	MW	235
Efficiency	%	90
The useful heat output	MW	529
Fuel consumption	kg/s	71.3
Mass flow of live steam/superheated steam	kg/s	185.4/165.5
Temperature of live steam	K	813
Pressure of live steam	MPa	13.17
Temperature in convection pass		
Inlet (before RH2)	K	1163
Before SH3	K	1028

Table 2. Operational parameters of the 235 MW_e CFB boiler.

Component			Component		
Fuel			Sorbent		
C	%	28.90	$CaCO_3$	%	92.0
H	%	2.60	$MgCO_3$	%	2.5
S	%	0.29	Inert	%	4.5
N	%	0.33	Moisture	%	1.0
O (by diff.)	%	6.78			
Moisture	%	40.90			
Ash	%	20.20			
HHV	kJ/kg	10,937.00			

The cleaning of heated surfaces in the convection pass of the boiler is carried out using steam and acoustic dust blowers of the Nirafon NI-100SS type depicted in Figure 4 with operating parameters shown in Table 3.

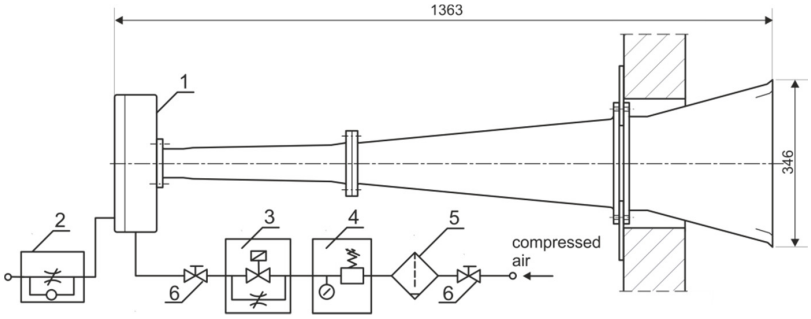

Figure 4. Schematic diagram of the Nirafon NI-100SS used in experimental tests. 1—Nirafon NI-100SS, 2—restrictor valve, 3—solenoid valve with bypass, 4—pressure regulator, 5—filter with water separator, 6—cut-off valves.

Table 3. Technical specification of acoustic cleaner Nirafon NI-100SS.

Frequency	100 Hz
Sound pressure level	approx. 150 dB (at the distance of 1 m from NI-100)
Compressed air:	
pressure	0.6 MPa
consumption	0.04 nm^3/s cleaning mode; 0.002 nm^3/s cooling mode
Material	SS 2343 (DIN 17445); (max. 800 °C)

The sound fields of the measurement space were analyzed in great detail in the design stage of the flue gas cleaning system. The result is the arrangement of devices in a convection cage shown in Figure 5, as well as an optimally selected regime of the work. The surface of the heat exchanger pipes is cleaned using an acoustic wave in the clearance area between the convection bundles of RH2 and SH3 superheater pipes. The cross-sectional area of the working zone is 20.266 × 8.724 = 176.8 m^2.

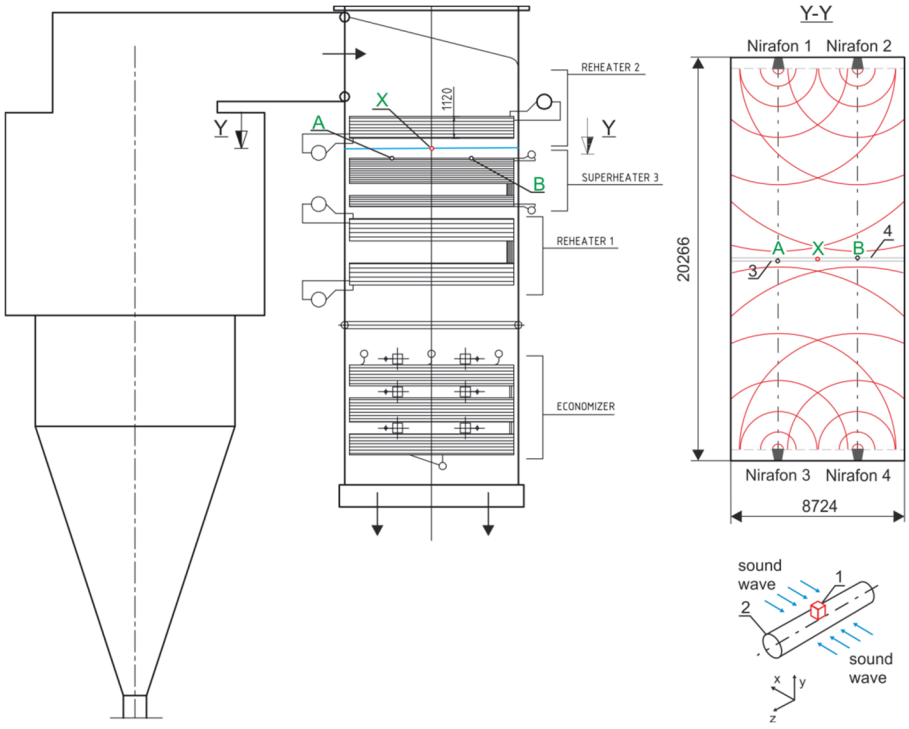

Figure 5. Schematic arrangement of acoustic dust blowers in the convection pass of the 235 MW_e CFB boiler operated in the PGE GiEK S.A. Turów Power Plant: 1—accelerometer, 2—pipe of superheater SH3, 3—pipe of superheater SH3 on which the sensor A is mounted, 4—pipe of superheater SH3 on which the sensor B is mounted, A, B—location of accelerometers ICP, Triaxial, 356A16, X—location of the microphone G.R.A.S. 40BH.

As can be seen from Table 3 and Figure 4, the blowers are constructed as a horn loudspeaker made of high-temperature resistant material SS2343 (max. 800 °C) and supplied with compressed air used for both cleaning and cooling of the equipment membrane. The blowers are operated by impulse. The typical pulse length of the sound emission is t_{imp} = 4 s and can be set within 1 and 30 s. The interval between sound emissions is t_p = 1 s and can be changed between 2 and 5 s, whereas the time interval between the sound emission sequences is t_s = 5 min and can be changed between 1 and 60 min.

3. Methods and Measurement Equipment

For the vibration measurement of SH3 steam superheater pipes, two ICP ceramic accelerometers Triaxial, 356A16 by PCB Piezotronics, placed at locations A and B (see Figure 4) on the top wall of the adjacent pipes were used. As can be seen from Figure 4, acoustic blowers generate sound waves perpendicular to the direction of the steam superheater pipes. An acceleration measurement has been carried out in three directions. The technical parameters of the accelerometers are presented in Table 4.

Table 4. Technical specification of accelerometer, ICP, Triaxial, 356A16.

Accelerometer, ICP, Triaxial, 356A16	
Sensitivity (±10%)	10.2 mV/(m/s^2)
Measurement Range	±490 m/s^2
Frequency Range (±5%) (y or z axis)	0.5 Hz to 5000 Hz
Frequency Range (±5%) (x axis)	0.5 Hz to 4500 Hz
Frequency Range (±10)	0.3 to 6000 Hz
Sensing Element	ceramic

During the measurements, the sound pressure level was also recorded at location 'X' (see Figure 4). For this purpose, the 1/4" G.R.A.S. type 40BH microphone was used, coupled with a preamplifier type 26AC. The used microphone had an extended measuring range up to 194 dB and allowed for linear measurement of sound intensity within the range from 10 Hz to 15 kHz. Detailed technical data of the microphone and preamplifier are shown in Tables 5 and 6, respectively.

Table 5. Technical data of high-pressure Microphone G.R.A.S. type 40BH.

$\frac{1}{4}$" G.R.A.S. Type 40BH Microphone	
Frequency range	10 Hz–20 kHz ± 2 dB
Upper limit of dynamic range	194 dB
Nominal Sensitivity	0.4 mV/Pa
Capacitance	6 pF
Temperature range	−40 °C do + 150 °C

Table 6. Technical data of the G.R.A.S. type 26AC preamplifier.

$\frac{1}{4}$" Preamplifier G.R.A.S. Type 26AC	
Frequency range	2.5 Hz–200 kHz ± 0.2 dB
Slew rate	20 V/µs
Input impedance	20 GΩ, 0.5 pF
Output impedance (Cs = 20 pF, f = 1 kHz)	75 Ω

For the acquisition of signals derived from the microphone and accelerometers, an 8-channel LMS V8-E measuring card was used. The device can be operated with a 24-bit signal processing and a sampling frequency of 204.8 kHz/channel. The measuring card was built in the LMS SCM01 module and cooperated with the LMS Test.Lab 11B software. In each of the analyzed cases, the work of the blowers was triggered manually and lasted about 1 s. The tests were carried out several times and the results of measurements presenting the most unfavorable case were analyzed.

4. Results

4.1. Measurements of Acoustic Pressure

Figure 6 presents the time variation of sound pressure measured in the central part of the convection cage (measurement point 'X'—see Figure 5) between the superheater SH3 and the reheater RH2.

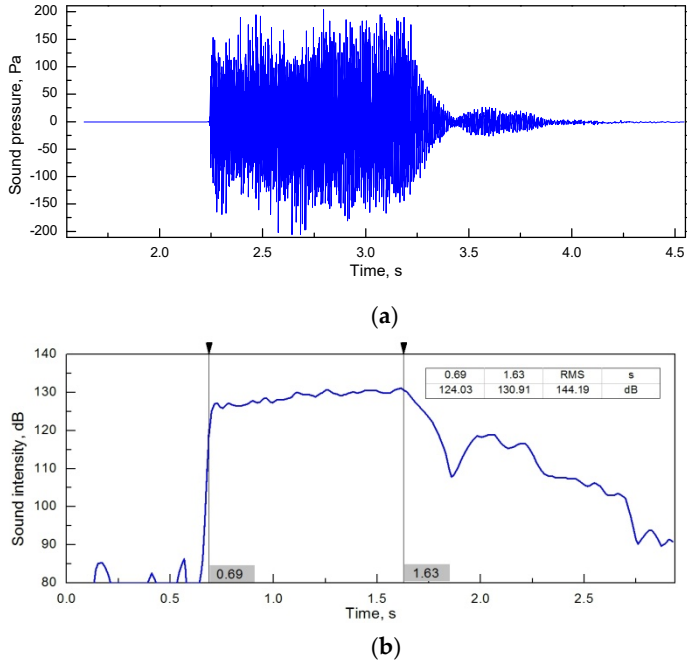

Figure 6. Time variation of sound pressure (**a**) and sound intensity (**b**) emitted by sonic soot blowers in the central part of the superheater SH3 (measurement point 'X'—see Figure 4).

As can be observed from Figure 6, the maximum sound pressure value does not exceed 200 Pa, and the root mean square (RMS) value of acoustic pressure recorded in the time interval from 0.69 to 1.63 s is 144.19 dB. Considering the parameters of the acoustic cleaners depicted in Table 1, this value is relatively low and may not be sufficient for effective cleaning of the SH3 superheater heating surfaces. However, keeping in mind the construction of the measuring space, the non-axial setting of the microphone, and the much greater distance of the measuring point from the sound source, the measured value of the sound intensity can be considered high. As the efficiency of the sonic soot blower action is the highest in the range of low sound wave frequencies, the sound intensity measurements should be complemented by the spectral analysis of the recorded sonic waves.

4.2. Acoustic Wave Spectral Analysis

Figure 7 presents the frequency spectrum of the acoustic wave generated by the sonic soot blowers in the central part of the convection cage of the superheater SH3 and the reheater RH2 (measurement point 'X'—see Figure 5). For analysis, a third-octave filter was used.

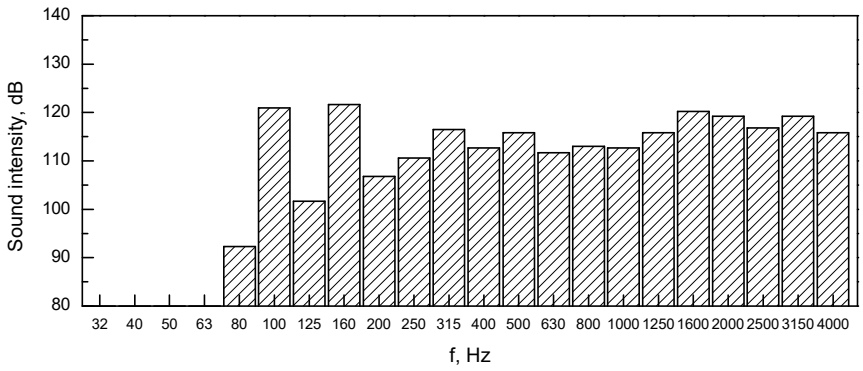

Figure 7. Frequency spectrum of the sound wave generated by the sonic soot blowers in the convection cage of the superheater SH3 and the reheater RH2 at the measurement point 'X' (see Figure 5).

As shown in Figure 7, contrary to what has been presented in the technical parameters (see Table 3), the Nirafon NI-100SS does not generate an acoustic wave with one frequency of 100 Hz, but a wave in the range from 80 to 4000 Hz. Moreover, as it can be seen from the spectral distribution, the intensity of the sound for the frequency of 100 Hz is close to that of the frequencies in the upper band (1600, 2000, and 3150 Hz). This means that the device generates a wave of high energy in the frequency range, which is irrelevant in the process of breaking the dust interparticle bond strength forces. Additionally, as shown in Figure 7, the maximum measured acoustic pressure level falls to the frequency of 160 Hz and amounts to ca. 122 dB. Similar values were also recorded for a frequency of 100 Hz. This suggests that despite the high RMS value of the sound generated by the sonic soot blowers (see Figure 6) for the frequency of 160 Hz, the energy carried by the acoustic wave is too low for breaking the dust adhesion forces. This was confirmed by the unilateral tangential ash deposits accumulated on the RH3 reheater's tubes, depicted in Figure 8.

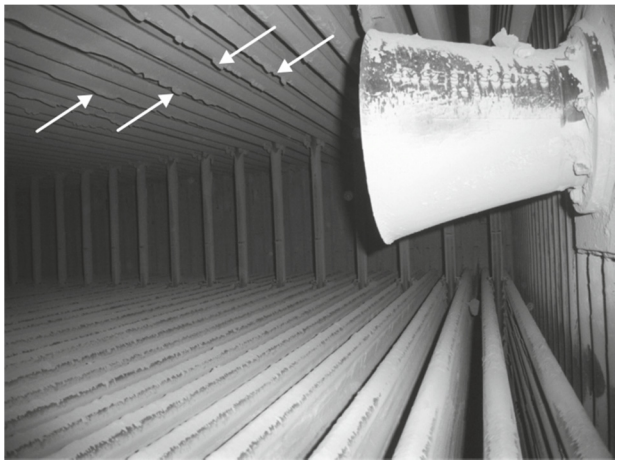

Figure 8. Convection cage of the 235 MW_e CFB boiler reheater. Arrows indicate ash deposits located on the pipes.

4.3. Measurements of Accelerations

Figures 9 and 10 show the acceleration time waveforms recorded for directions x, y, and z in points A and B of the measurement space (see Figure 5). As is shown in Figures 9 and 10, the highest acceleration values (9.43 m/s^2 and 7.38 m/s^2) occur in the direction consistent with the direction of acoustic wave propagation, that is, direction x transverse to the axis of superheater pipes.

On the other hand, the smallest value (3.54 m/s^2) is recorded in the direction transverse to the direction of the wave propagation (i.e., z direction), following the superheater pipe axis direction. The maximum acceleration values recorded in the y and z directions are smaller compared to the value recorded in the x direction by 54 and 60%, respectively. For the accelerometer located at point B, these values are smaller at 27% for the y direction and 36% for the z direction.

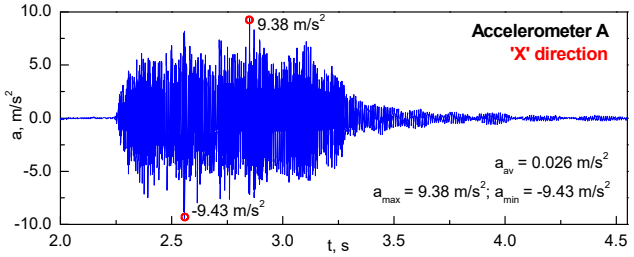

(**a**)

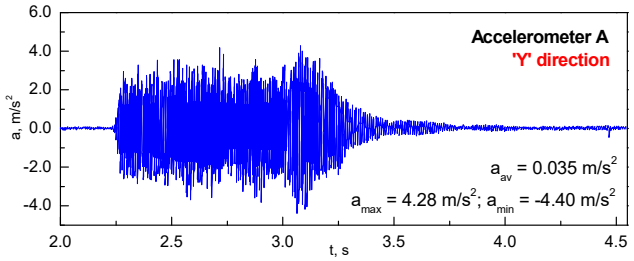

(**b**)

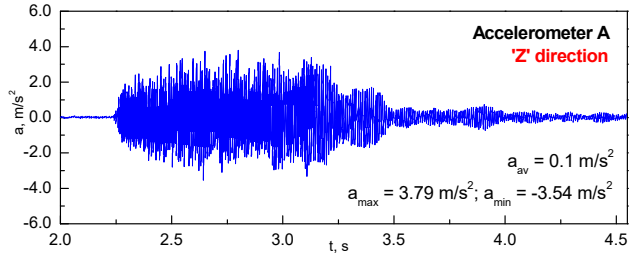

(**c**)

Figure 9. Time variation of a measured acceleration in point A, for: (**a**) x, (**b**) y, and (**c**) z directions.

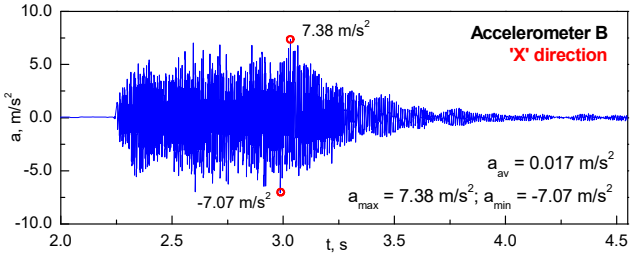

(**a**)

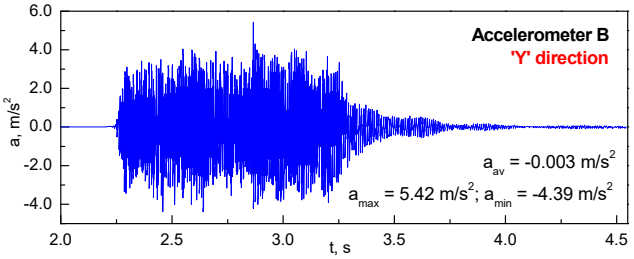

(**b**)

Figure 10. *Cont.*

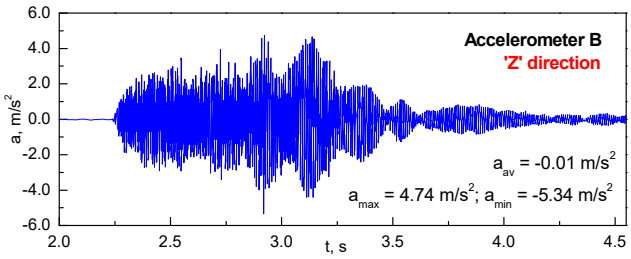

(**c**)

Figure 10. Time variation of a measured acceleration in point B, for: (**a**) x, (**b**) y, and (**c**) z directions.

4.4. Calculations of Displacement

For continuous functions, the basis for determining of displacement $d(t)$ from a measured acceleration $a(t)$ can be obtained from the following mathematical formula

$$d(t) = d_0 + v_0 t + \int \left(\int a(t)dt \right) dt, \tag{1}$$

where: d_0—initial displacement, m; $t = 0$, v_0—initial velocity, m/s; $t = 0$

The integration of a recorded (discrete) signal in the time domain is calculated numerically from the following correlation

$$\int_0^n a(t)dt \cong \sum_{i=1}^{n} \left(\frac{a(i-1) + a(i)}{2} \right) \Delta t, \tag{2}$$

where: $a(i)$—i-th sample of the time waveform; Δt—time increment between samples t_{i-1} and t_i; n—number of samples.

As follows from Equation (1), displacement must be calculated in two steps, first computing velocity from acceleration, and then displacement from velocity. Thus, for a discrete signal of a measured acceleration, displacement can be calculated based on the following equation

$$d(t) = \lim_{n \to \infty} \sum_{i=1}^{n} \sum_{i=1}^{n} a(t_i) \Delta t. \tag{3}$$

It should be noted that double integration of the input signal generates the constant component in each integration. As a result, the calculated velocity time waveforms may be offset from the real waveforms, resulting in a displacement time series that increases with time. As has been pointed out by Rocha et al. [13] these errors can be corrected by applying the correct initial condition for the numerical simulation or by application of a high-pass filter. In this work, the second method is used. In the process of displacement calculation, the Vibrationdata Matlab Signal Analysis and Structural Dynamics Package and in-house algorithms have been used. Based on the recorded acceleration time waveforms, the pipe displacements were determined, which are shown for the individual accelerometers in Figures 11 and 12.

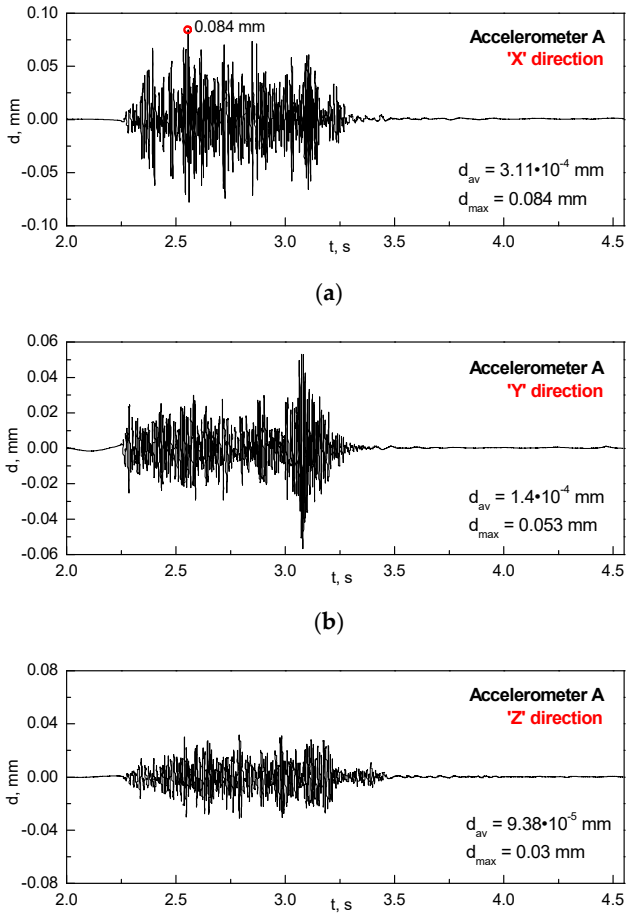

Figure 11. Time variation of the SH pipe displacements measured by accelerometers in measurement point A for: (**a**) x, (**b**) y, and (**c**) z directions.

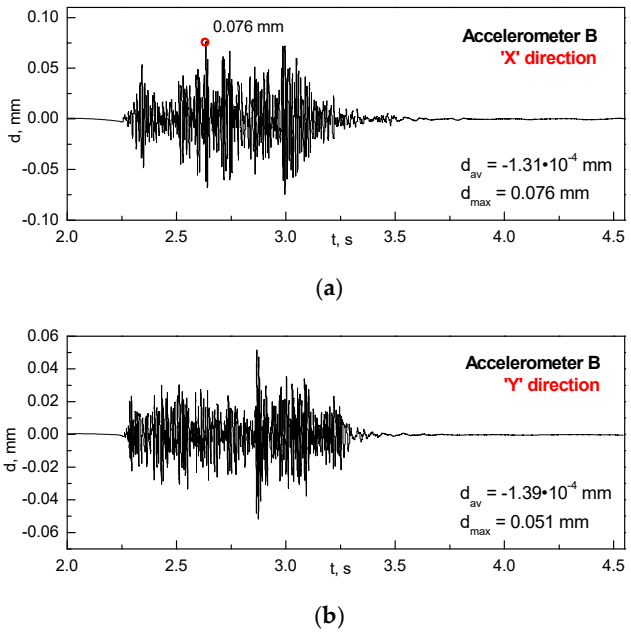

Figure 12. *Cont.*

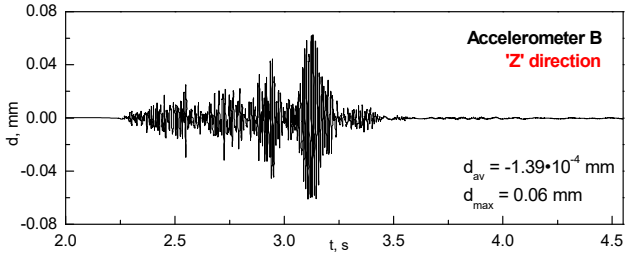

(**c**)

Figure 12. Time variation of the SH pipe displacements measured by accelerometers in measurement point B for: (**a**) x, (**b**) y, and (**c**) z directions.

As can be seen in the Figures, the maximum vibration amplitudes of the steam superheater pipes occur in the x direction perpendicular to the direction of propagation of the acoustic wave, with the values being small and not exceeding 87 μm. This means that the energy carried by the acoustic wave generated by the sonic soot blowers is safe for the superheater pipes and will not be destructive in any way. This thesis is confirmed by the long-term and failure-free operation of acoustic blowers for superheater pipes, as well as much larger permissible amplitude of their vibrations in the normal state of the boiler operation ($d \leq 5$ mm). It is worth noting that such small values of vibration amplitudes are the effect of stiffening of the superheater pipes, which are mounted in the middle of the convection cage. The results obtained, therefore, relate to the vibrations of the superheater pipe mounted approx. 4 m between two fixed support points. Since the tests were conducted during the boiler shutdown, measured amplitudes of the SH3 tube vibrations were caused only by the impact of acoustic blowers. Therefore, during the normal operation of the boiler, periodically higher vibration amplitudes should be expected. For this reason, the results obtained in this study should be interpreted as an answer to the question: what is the contribution of the acoustic blowers to the mechanical process of cleaning the superheater pipe surface from ash deposits? It is noteworthy that during normal boiler operation, better cleaning of the SH3 heating surfaces is to be expected as a result of the acoustic wave emitted by the soot blowers. This is due to several reasons. First, in this condition, the fly ash is transported in the hot flue gas stream so that the energy of the acoustic wave is not lost to breaking interparticle bond strength forces and can be fully utilized to increase the turbulence of the gas–solid flow. Secondly, during normal boiler operation, the superheater tube vibration amplitude is a superposition of the natural vibrations caused by the auxiliary equipment operating in the second pass and the vibrations caused by the acoustic blowers.

Figure 13 shows a comparison of maximum accelerations and displacements of superheater pipes SH3 in all analyzed directions measured at measurement points A and B.

As can be seen from the Figure, the vibration amplitudes of the SH3 superheater pipes in the 'x' and 'y' direction recorded by the accelerometers are comparable. This confirms the symmetrical distribution of the acoustic wave generated by the sonic soot blowers in the measurement space. The greatest difference occurs in the axial direction of the pipes, where in the case of accelerometer B, almost two times greater displacements were recorded.

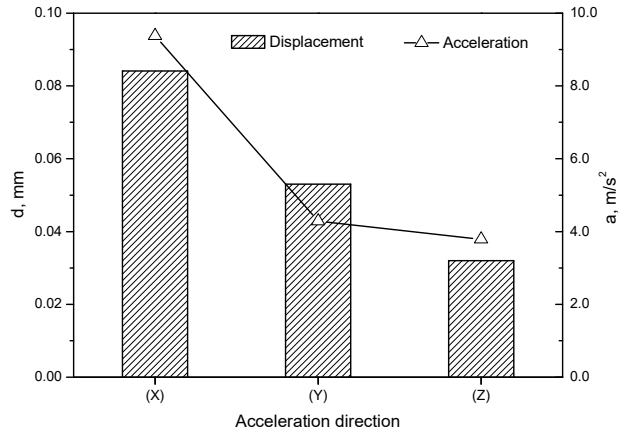

(**a**)

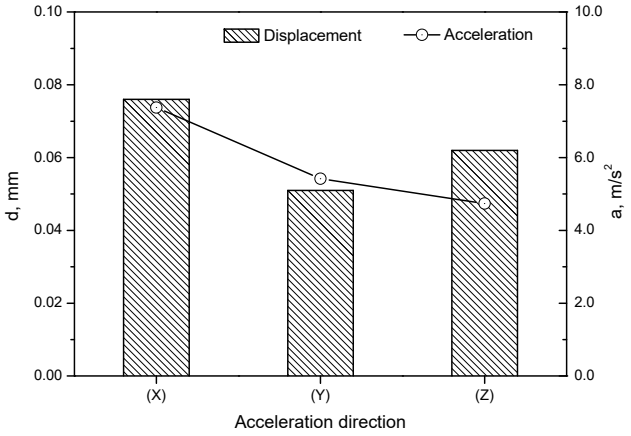

(**b**)

Figure 13. Summary of maximum accelerations and displacements measured by accelerometers in measurement points: (**a**) A and (**b**) B in x, y, and z directions.

5. Concluding Remarks

The conducted tests of vibrations of the SH3 superheater pipes caused by the acoustic waves of the sonic soot blowers resulted in the following conclusions:

(a) The acoustic energy generated by the sonic soot blowers in the center of the measurement space is high, but does not exceed 150 dB. Considering the size of the convection cage, as well as the specific properties of fly ash from lignite combustion, the energy of the acoustic waves is not sufficient to clean the surfaces of the RH2 and SH3 superheaters effectively.

(b) The maximum sound pressure values corresponding to 100 and 160 Hz wave frequencies do not exceed 122 dB. This means that for the design frequency of 100 Hz, the sonic soot blowers do not generate a wave pressure of 150 dB.

(c) The highest acceleration values are in the direction consistent with the direction of the acoustic wave propagation, that is, the 'x' direction transverse to the axis of the superheater pipes.

(d) The maximum vibration amplitudes of the superheater pipes are perpendicular to the direction of the acoustic wave propagation and reach very small values not exceeding 87 μm. The small vibration values result from the stiffening of the superheater pipes mounted in the middle of the pipe length.

The conducted measurements confirmed the assumption that comprehensive studies of vibrations of CFB boiler steam superheater tubes caused by the operation of acoustic dust blowers must include both acoustic and vibration measurements. Acoustic measurements using a specially designed microphone with an extended measuring range allowed to assess the performance of devices generating high energy waves, while triaxial acceleration sensors provided the possibility of indirectly assessing the amplitude of vibrations. Taking all into account, it should be concluded that the use of high-energy acoustic waves to clean the surface of the superheaters RH2 and SH3 does not risk damage to the pipes. Thus, the direct impact of the acoustic wave to break the dust interparticle bond strength forces will be decisive for the effectiveness of cleaning the contaminated surfaces with a fly ash. However, it should be emphasized that due to the direct relationship between the geometry of the chamber in which the acoustic wave propagates and the effectiveness of ash pollution removal, the use of acoustic blowers in CFB boilers must be preceded by a thorough analysis of the acoustic field of the chamber in which the system will operate.

Funding: The scientific research was funded by the statute subvention of Czestochowa University of Technology, Faculty of Infrastructure and Environmental.

Conflicts of Interest: The author declares no conflict of interest.

Nomenclature

a_{av}	average acceleration (m/s^2)
a_{max}	maximum acceleration (m/s^2)
a_{min}	minimum acceleration (m/s^2)
$a(i)$	i-th sample of the time waveform (m/s^2)
d_{av}	average displacement (m)
d_{max}	maximum displacement (m)
d_{min}	minimum displacement (m)
d_0	initial displacement (m)
d_{32}	Sauter mean particle diameter (m)
d_{50}	mass mean particle diameter (m)
f	frequency (Hz)
n	number of samples (-)
U_0	superficial gas velocity (m/s)
U_{mf}	minimum fluidization velocity (m/s)
t	time (s)
Δt	time increment between samples t_{i-1} and t_i (s)
v_0	initial velocity (m/s)

Abbreviations

HHV	High Heating Value
RH	Reheater
RMS	Root Mean Square
SH	Superheater

References

1. Pophali, A.; Emami, B.; Bussmann, M.; Tran, H. Studies on sootblower jet dynamics and ash deposit removal in industrial boilers. *Fuel Process. Technol.* **2013**, *105*, 69–76. [CrossRef]
2. EPRI. *Ash Deposition Impacts in Power Industry, Research Project No. 1010315*; EPRI: Palo Alto, CA, USA, 2006.
3. Moskal, T.; Scott, S. *Economic Consequences of Boiler Cleaning Effectiveness, Technical Publication #DPTP-98-1*; Diamond Power International: Lancaster, OH, USA, 1998.
4. Gupta, R.P.; Rushdi, A.; Browning, G.J.; Wall, T.F. A Mechanistic Approach for Assessing Thermal Performance of Coal Blends. In Proceedings of the Power Production in the 21st Century: Impact of Fuel Quality and Operations Conference, Snowbird, UT, USA, 26–31 October 2001.
5. Skea, A.; Bott, T.R.; Beltagui, S.A. A comparison of mineral fouling propensity of three coals using a pilot scale under-fed stoker combustor. *Appl. Therm. Eng.* **2002**, *22*, 1835–1845. [CrossRef]
6. Zbogar, A.; Frandsen, F.; Jensen, P.A.; Glarborg, P. Shedding of ash deposits. *Prog. Energy Combust. Sci.* **2009**, *35*, 31–56. [CrossRef]

7. Peña, B.; Teruel, E.; Díez, L.I. Towards soot-blowing optimization in superheaters. *Appl. Therm. Eng.* **2013**, *61*, 737–746. [CrossRef]
8. Peña, B.; Teruel, E.; Díez, L.I. Soft-computing models for soot-blowing optimization in coal-fired utility boilers. *Appl. Soft Comput.* **2011**, *11*, 1657–1668. [CrossRef]
9. Shi, Y.; Wang, J.; Liu, Z. On-line monitoring of ash fouling and soot-blowing optimization for convective heat exchanger in coal-fired power plant boiler. *Appl. Therm. Eng.* **2015**, *78*, 39–50. [CrossRef]
10. Kumari, S.A.; Srinivasan, S. Ash fouling monitoring and soot-blow optimization for reheater in thermal power plant. *Appl. Therm. Eng.* **2019**, *149*, 62–72. [CrossRef]
11. Wojnar, W. Erosion of heat exchangers due to sootblowing. *Eng. Fail. Anal.* **2013**, *33*, 473–489. [CrossRef]
12. Hare, N.; Rasul, M.; Moazzem, S. A review on boiler deposition/foulage prevention and removal techniques for power plant. In *EE'08 Proceedings of the Recent Advances in Energy and Environment Conference, IASME/WSEAS International Conference on Energy and Environment, Cambridge, UK, 23–25 February 2010*; Rosen, A., Krope, J., Garbai, L., Kozic, D., Goricanec, D., Sakellaris, I., Eds.; WSEAS Press: Stevens Point, WI, USA, 2010; pp. 217–222.
13. Rocha, S.M.S.; Feiteira, J.F.S.; Mendes, P.S.N.; Da Silva, U.P.B.; Pereira, R.F. Method to Measure Displacement and Velocity from Acceleration Signals. *Int. J. Eng. Res. Appl.* **2016**, *6 Pt 4*, 52–59.